Journal of Medicinal Chemistry

Article

pubs.acs.org/jmc

Integrated Virtual Screening for the Identification of Novel and Selective Peroxisome Proliferator-Activated Receptor (PPAR) Scaffolds

Daniel K. Nevin,[†] Martin B. Peters,[‡] Giorgio Carta,[†,§] Darren Fayne,[†] and David G. Lloyd*[,†]

[†]Molecular Design Group, School of Biochemistry and Immunology, Trinity Biomedical Sciences Institute, Trinity College Dublin, Dublin 2, Ireland

[‡]Irish Centre for High-End Computing (ICHEC), Tower Building, Trinity Technology and Enterprise Campus, Grand Canal Quay, Dublin 2, Ireland

Supporting Information

ABSTRACT: We describe a fully customizable and integrated target-specific "tiered" virtual screening approach tailored to identifying and characterizing novel peroxisome proliferator activated receptor γ (PPARγ) scaffolds. Built on structure- and ligand-based computational techniques, a consensus protocol was developed for use in the virtual screening of chemical databases, focused toward retrieval of novel bioactive chemical scaffolds for PPARγ. Consequent from application, three novel PPAR scaffolds displaying distinct chemotypes have been identified, namely, 5-(4-(benzyloxy)-3-chlorobenzylidene)dihydro-2-thioxopyrimidine-4,6(1*H*,5*H*)-dione (MDG 548), 3-((4-bromophenoxy)methyl)-*N*-(4-nitro-1*H*-pyrazol-1-yl)benzamide (MDG 559), and ethyl 2-[3-hydroxy-5-(5-methyl-2-furyl)-2-oxo-4-(2-thienylcarbonyl)-2,5-dihydro-1H-pyrrol-1-yl]-4-methyl-1,3-thiazole-5-carboxylate (MDG 582). Fluorescence polarization (FP) and time resolved fluorescence resonance energy transfer (TR-FRET) show that these compounds display high affinity competitive binding to the PPARγ-LBD (EC_{50} of 215 nM to 5.45 μM). Consequent characterization by a TR-FRET activation reporter assay demonstrated agonism of PPARγ by all three compounds (EC_{50} of 467−594nM). Additionally, differential PPAR isotype specificity was demonstrated through assay against PPARα and PPARδ subtypes. This work showcases the ability of target specific "tiered screen" protocols to successfully identify novel scaffolds of individual receptor subtypes with greater efficacy than isolated screening methods.

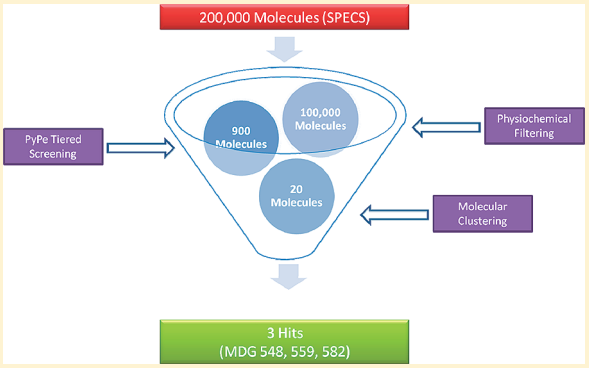

INTRODUCTION

Peroxisome proliferator-activated receptors (PPARs) are ligand activated transcription factors that form a subfamily of the nuclear receptor superfamily. PPARs form heterodimers with the 9-*cis*-retinoic acid receptor (RXR) and activate transcription events by binding to a specific DNA element called the PPAR response element (PPRE).[1] Their transcription factor activity accounts for a wide range of effects on metabolism, cellular proliferation, cellular differentiation, and immune responses.[2] From a pathological perspective, PPARs are implicated in a diverse range of disease states including type II diabetes, obesity, dyslipidemia, atherosclerosis, inflammation, and neurodegeneration.[3−9] Presently, numerous studies have undertaken a computational approach to drug design for PPARγ. Application of ligand- and/or structure-based computational methods has led to the discovery of diverse compound classes targeting these nuclear receptors.[10−14]

Previous work by our group has shown the beneficial application of target specific and tiered screen modeling approaches to novel hit identification in nuclear receptors.[15−17] Accordingly, to extend our investigation to PPARγ, we again undertook to apply a combination of complementary in silico methodologies and in vitro biochemical techniques tailored for the identification and validation of novel scaffolds for these nuclear receptors. Building on earlier studies, we parametrized and validated individual components of a PPAR-focused virtual screening protocol. These components were integrated in a tiered screen protocol and used to virtually predict novel scaffolds with affinity or selectivity for PPARγ from commercial compound vendor databases.

An in-house virtual screening platform was developed called PyPe (parallel Python Pipeline) that incorporates both propriety and open source computational tools to provide a highly customizable, fast, and homogeneous environment for virtual high throughput screening (vHTS). The tiered screen protocol was constructed and run using this platform. From a database of approximately 200 000 molecules, a total of

Received: November 11, 2011
Published: May 14, 2012

   dx.doi.org/10.1021/jm300068n | *J. Med. Chem.* 2012, 55, 4978−4989

20 compounds were identified as putative (virtual) hits. Through the use of biochemical competitive binding techniques, three compounds were confirmed with micromolar (0.25−5.45 μM) binding affinity to PPARγ-LBD. Importantly, PPAR isotype selectivity studies identified one compound as a PPARγ specific scaffold **1** (MDG 548), one as a pan-PPAR isotype compound **2** (MDG 559), and a dual targeting PPARδ/γ agent **3** (MDG 582). The compounds identified present novel chemotypes not previously reported as having activity against these PPAR receptor targets. Our work also demonstrates the utility of a tiered screening model that shows greater screening efficacy against PPARs than can be achieved through use of the discrete methods used alone.

RESULTS

Protein Receptor Selection, Preprocessing, and Protein−Ligand Interaction Fingerprint (PLIF) Analysis. At the time of study, 98 PPAR X-ray crystal structures were present in the Protein Data Bank (PDB). Of this number, 73 structures were of PPARγ, of which 69 were cocrystallized with a bound druglike molecule. In order to further stratify this data set, PLIF analysis was used to map the protein−ligand interactions profiles observed. A group of 22 structures was selected (see Supporting Information Table S1) for consideration in structure-derived pharmacophore model generation. All 22 structures were included in a conformational analysis and validation study (group A). The inclusion of a broad spectrum of cocrystallized chemotypes provided a sufficient span for PPAR ligand conformational space exploration. A 12-member subset of group A ligands was used for consensus pharmacophore query generation (group B). These compounds showed conservation of the hydrogen bond interaction profile exhibited by the PPARγ agonist rosiglitazone (hydrogen bonding at Ser289, His323, His449, and Tyr473).

Conformer Generation: Method Comparison and Validation. To compare the ability of OMEGA and MOE (stochastic/LowModeMD) to reproduce ligand bioactive conformations, a comparison of the lowest rmsd conformations generated to the actual crystal pose was investigated for the group A ligands. Method comparison showed little variation in the lowest rmsd to bioactive conformation obtained (see Supporting Information Table S2). OMEGA (average lowest rmsd of 0.92) outperformed MOE LowModeMD (average lowest rmsd of 0.96) and MOE stochastic (average lowest rmsd of 1.03). As the difference between generation methods was marginal, the computational calculation time for our systems was also accounted for each method. OMEGA completed its conformer generation steps on the ligand set in a relatively short period of time, whereas both MOE methods were significantly longer. As all programs were run under the same computing conditions, OMEGA was chosen for use within this study because of its performance in bioactive pose reproduction and its lower CPU clock time.

Building on previous work by our group,[18] we undertook parametrization of OMEGA settings from default. The effect of varying the max confs (maximum conformations) setting in OMEGA was investigated. In all instances, a maximum number of conformers enumerated by OMEGA for each ligand was reached within a max confs setting of n = 10000. For 8 out of 22 ligands, we observed no appreciable improvement in rmsd on variation of max confs settings. For this ligand subset, the conformer with the lowest rmsd was within the first 100 conformers generated. For the other 14 ligands, an improvement in rmsd relative to the bioactive pose was observed, validating an increase of the parameters beyond default.

For these ligands, convergence of the lowest average rmsd obtained (rmsd = 0.94) was met at a max confs setting of n = 1000. Increased settings to n = 5000 or n = 10000 did not significantly improve the average rmsd score for conformations retrieved.

Pharmacophore Modeling. We sought to assess the performance of a MOE consensus pharmacophore model generated from the group B ligand set. On initial inspection of the performance of an autogenerated query (default settings), a large degree of ambiguity existed in the features defined by the consensus pharmacophore creator. This lack of clarity in feature definition was likely correlated to the chemodiversity of the ligand set. Consequently, the automatically generated pharmacophore was considered unsuitable for use in PPARγ modulator virtual screening. To simplify and refine the query, while retaining high confidence in its derivation, a manual query was created from a single potent PPARγ agonist (rosiglitazone) and assessed against a validation screening set.

The PPARγ-LBD bound conformation of rosiglitazone (PDB code 1FM6) was selected as the model template ligand (Figure 1).

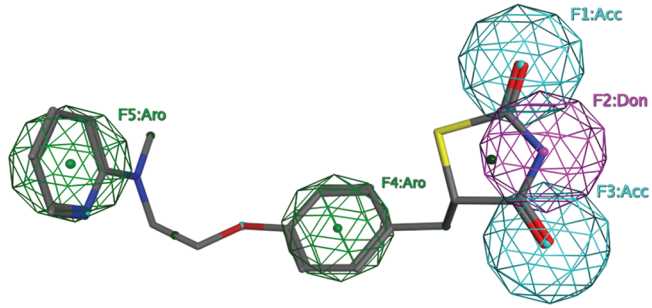

Figure 1. Hypo 1 pharmacophore query: five-point pharmacophore query modeled on the bioactive conformation of rosiglitazone within the PPARγ-LBD. Three features are located on the TZD headgroup, with two aromatic features mapped onto core and tail aromatic regions of the molecule: Acc, acceptor; Don, donor; Aro, aromatic. The figure was generated using MOE (version 2010.10).

Use of the pharmacophore query editor program in MOE attributed 11 potential pharmacophoric features from the ligand. In order to reduce the feature list, pharmacophoric points informed by the earlier PLIF analysis were selected in the first instance, including the three pharmacophore points known to be involved in hydrogen bonding within the PPARγ LBD. All three features (F1, F2, and F3) were mapped onto the thiazolidinedione (TZD) region of the ligand. In rosiglitazone, the carbonyl oxygen (mapped onto the F1 feature) participates in hydrogen bonding with His499. F2 was defined as a hydrogen bond donor and is known to engage in hydrogen bonding with Tyr473 in the template ligand. F3 was also defined as an acceptor group, and the carbonyl oxygen is known to make two hydrogen bond interactions with Ser289 and His323. F4 and F5 were annotated as aromatic ring centers. This initial query was designated as Hypo 1, and multiple variants were assessed.

In total, 24 hypotheses (Hypo 1 to Hypo 23) were created (see Supporting Information Table S3). Each examined the effects of adjusting pharmacophore model parameters and assessing these changes in terms of the percentage of actives and decoys retrieved from a PPARγ DUD screening set. Ten

dx.doi.org/10.1021/jm300068n | J. Med. Chem. 2012, 55, 4978−4989

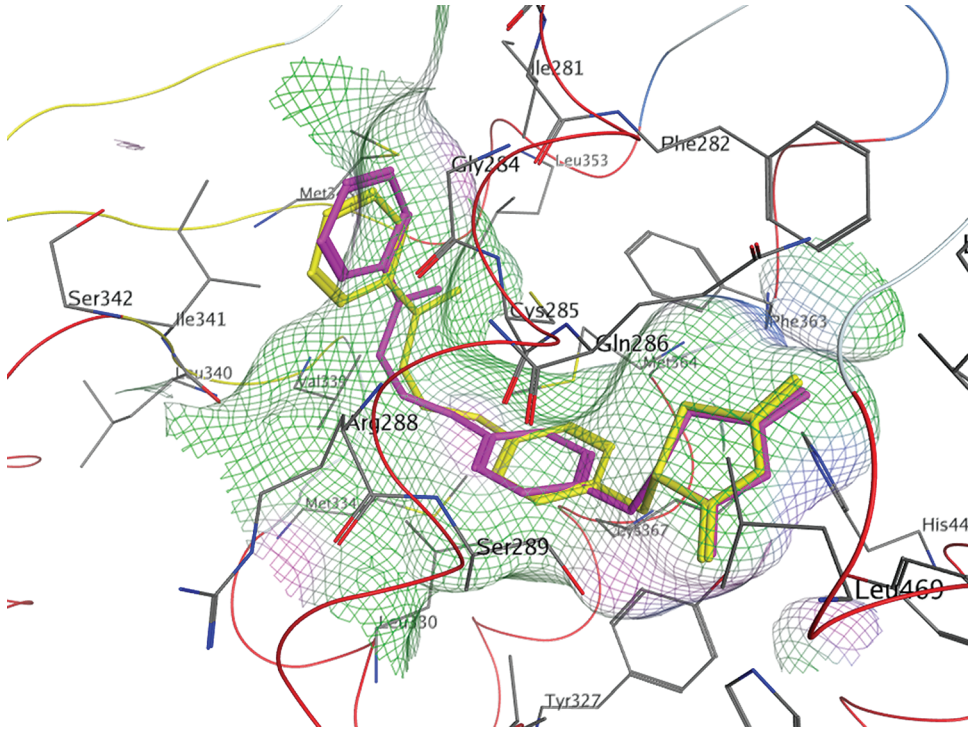

Figure 2. FRED docking validation: superimposition of the native (purple) and re-docked pose (yellow) of rosiglitazone within the PPARγ-LBD. The rmsd of docked bioactive conformer to the receptor bound ligand was calculated at 0.05 Å. The figure was generated using MOE (version 2010.10).

conditions examined inclusion of a sixth feature (PCH Hyd) in the model, but this inclusion did not yield improvement over Hypo 1. Hypo 1 successfully retrieved 83% of the actives group, while it retrieved only 21% of the decoy set. With a percent differential of 62%, indications show that this model is largely selective for PPARγ DUD set actives over decoy molecules. As the DUD database is based on physicochemical similarity between actives and decoys, this supports the idea that the model has the ability to separate the two groups based on their topological and presumed physiological differences. Multiple variations on the lead model did not result in an improvement in the percentage difference between actives and decoy retrieved (% actives − % decoys = % difference). Interestingly, Hypo 23 also retained a percentage difference of 62%. This model included explicit volume restrictions on where ligands were permitted to map within the pharmacophore model. However, Hypo 23 only allowed 66% of actives through versus 83% of Hypo 1. As the comparatively simpler Hypo 1 scored equally as well, it was chosen over Hypo 23 for inclusion in the tiered screen. The results of this study suggest that basing a pharmacophore model on a single validated PPARγ ligand affords a viable approach in the initial stages of a target-specific virtual screening protocol. As the DUD database active set displays topological diversity, it is encouraging that the uncomplicated 3D pharmacophore model can retrieve a high proportion of true positives/active compounds. Comparison of percentage differential was used as an initial validation metric. In tandem to this approach, pharmacophore models were also subjected to validation by ROC curve analysis on the models' performance against the PPARγ DUD database. The Hypo 1 pharmacophore model scored highly in its ability to distinguish actives from putative decoy molecules (AUC = 0.92).

Docking Validation. To validate use of FRED[19] within a tiered PPARγ virtual screening protocol, the ability of the program to reproduce bioactive ligand poses was examined. An evaluation of scoring functions applied to the comparative ranking of the bioactive conformation of rosiglitazone (PDB code 1FM6) to that of multiple conformations (n = 1000) showed that of those functions implemented in FRED, Chemgauss3 ranked the bioactive conformation first out of the conformational data set (Figure 2) docked. FRED/Chemgauss3 was selected for use in the docking aspects of the virtual screening protocol. The PPARγ DUD data set was docked into the PPARγ receptor, and output compound poses were ranked. ROC curve analysis, which assesses the ability of a model to distinguish actives from inactives, was used to assess the performance of the FRED protocol. The analysis shows that the model is able to successfully distinguish between known PPARγ actives and decoy molecules for the PPARγ DUD data set (AUC = 0.83). In a study carried out by Jain et al., the performance of another docking program (Surflex-Dock) on the PPARγ DUD data set was comprehensively evaluated and yielded similar values to those displayed by FRED (AUC = 0.88).[20]

ROCS: Query Creation and Validation. To assess the utility of ROCS, a shape-based comparison virtual screening program, in a tiered PPAR protocol, the PPARγ-LBD co-crystallized ligand GI262570 (PDB code 1FM9) was used as a shape template for a quantitative analysis. GI262570 was chosen because of its larger volume compared to rosiglitazone, thus potentially allowing larger molecules through a shape matching query. As PPARγ-LBD comprises a large binding cavity (~1300 Å^3), allowing for size diversity among screening molecules was seen as potentially advantageous. Comparison of ROCS scoring functions was performed analogously to that used for the FRED evaluation. The total set of ROCS scoring functions were analyzed and performance ranked (AUC). Results demonstrate that ColorTanimoto scoring function was

dx.doi.org/10.1021/jm300068n | J. Med. Chem. 2012, 55, 4978−4989

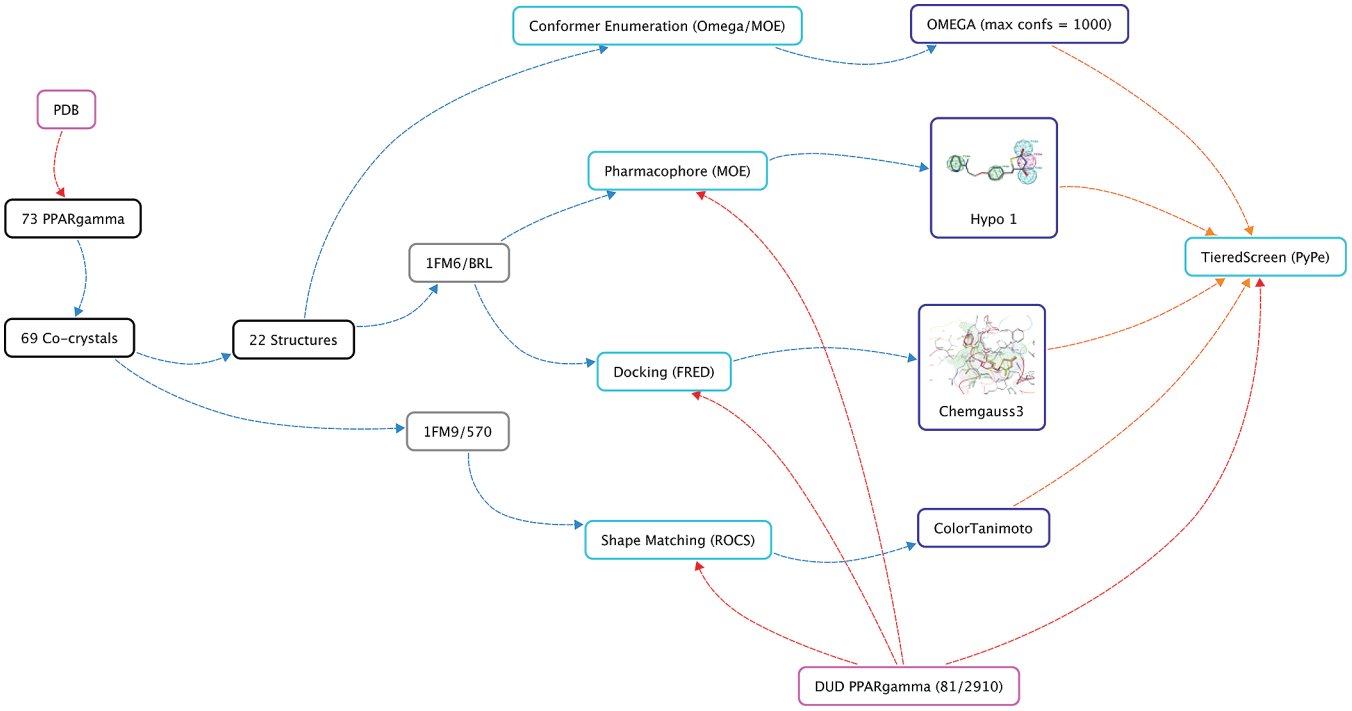

Figure 3. Validation workflow for tieredScreen model. Conformer generation, MOE pharmacophore, FRED docking, and ROCS shape matching were parametrized and validated against the PPARγ DUD set before incorporation into a tieredScreen model. Rosiglitazone in complex with PPARγ-LBD (1FM6/BRL) was used for manual pharmacophore generation and docking, while GI262570 in complex with PPARγ-LBD (1FM9/570) was used for shape matching query generation. Color coding is as follows: pink, databases; black, PDBs; gray, ligand−PPARγ complexes; cyan, programs used; purple, validation results.

best able to distinguish PPARγ actives over decoys (AUC = 0.95). Analysis revealed that 10 out of 13 ROCS scoring functions returned an AUC score of ≥0.92. RefTversky received an AUC of 0.808 while ShapeTanimoto and FitTversky received 0.77 and 0.72, respectively. ROCS/ColorTanimoto was accordingly selected for use within the protocol. Ligand-based virtual screening comparison work using the DUD PPARγ set returned similar results for the performance of ROCS[21] The data additionally suggest that use of a simple shape-based comparison method in PPARγ virtual screening is appropriate in either single or tiered virtual screen approaches.

Tiered Screening: Application and Validation. Figure 3 illustrates the component comparative studies of this investigation and their integration to a single tiered platform. To facilitate integration of the components, we advanced a bespoke, customizable parallel dataflow environment. Scripted in Python, PyPe functions analogously to environments such as Pipeline Pilot[22] and Knime.[23] Our aim here was to ascertain the benefit(s) of methodology integration over application of the individual methodologies for target-specific screening performance. Figure 5 illustrates the workflow integration employed to create the tiered screen platform in PyPe.

Analysis of the output showed that merging of the individual models into a tiered screening consensus model resulted in a selective and accurate virtual screening pipeline for PPAR (AUC = 0.80). Although the consensus score is derived from the average scores of each component of the tiered screen protocol (MOE Ph4, FRED, and ROCS), the AUC score obtained from this run is not simply an average of the AUCs obtained from the three validation steps carried out in earlier work. This arises from the fact that the pharmacophore search acts as a "master filter", where passed molecules are subsequently sent to FRED and ROCS for further interrogation. As validation of individual screening tools was carried out by the full (unfiltered) DUD set (82 actives/3112 decoys), this explains the differences arising in the ROC analysis.

Analysis of PPARγ DUD active/decoy hit lists from individual methods versus tiered screen results revealed several points of note. Analysis of negative predictive value (NPV) across screening methods revealed a high rate of negative prediction in all cases, with the tiered screen protocol marginally outperforming stand-alone methods (NPV values: tiered screen, 0.97; MOE Ph4, 0.91; FRED, 0.95; ROCS, 0.92). Regarding false positive rate (FPR) values obtained for the PPARγ DUD data set, ROCS retained the lowest rate (0.008) followed by tiered screen and FRED (both 0.021) and MOE Ph4 (0.024). Although ROCS performed better than tiered screen or FRED/MOE Ph4 with relation to FPR, the structural similarities between the PPARγ DUD set and model ligand used may account for this. Overall, it is believed that application of three screening methods simultaneously places more stringent filters on database virtual screening. Using a consensus method instills a higher level of confidence in the results, as all methods point in the same discovery direction. As initial hit list sizes can reach several thousand in a typical run, the application of rigorous filtering in the virtual screen can potentially reduce subsequent workload and facilitate chemotype scaffold hopping.

Figure 4 below describes the virtual screening workflow utilized. SPECS chemical vendor database was initially reduced to about 100 000 compounds through application of a set of PPARγ agonist physiochemical descriptors. The reduced compound list was then screened through the PyPe tiered screen, and a prioritized consensus scored (C_score) hit list of 900 compounds was retained. These compounds were clustered based on molecular similarity to furnish n = 20 clusters, affording chemotype diversity across the consensus

dx.doi.org/10.1021/jm300068n | J. Med. Chem. 2012, 55, 4978−4989

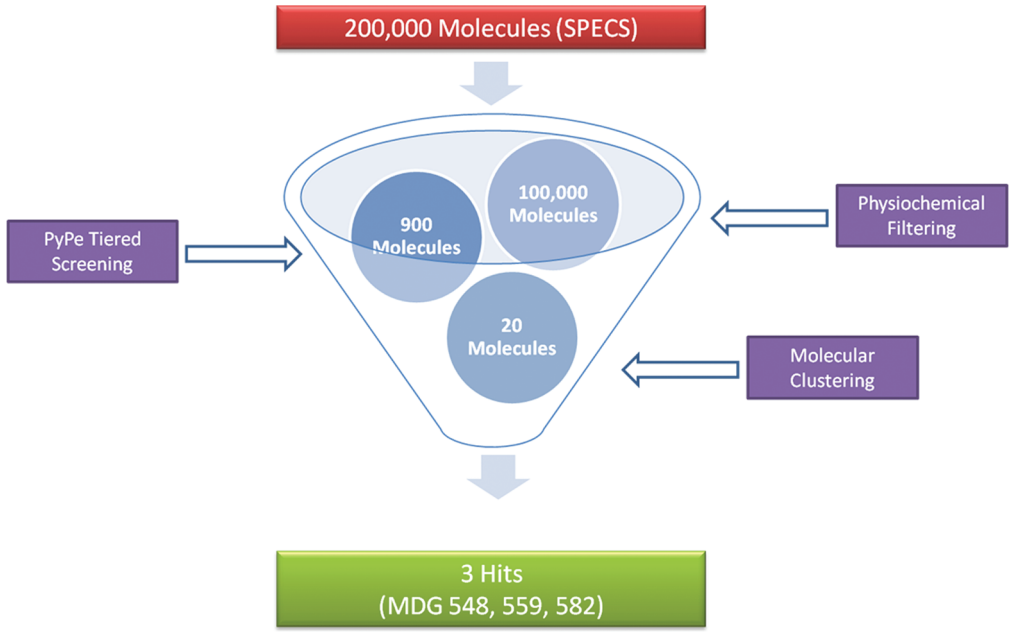

Figure 4. Virtual screening workflow. SPECS database was reduced from approximately 200 000 compounds to approximately 100 000 using a set of PPARγ-like physiochemical descriptor filters. Through PyPe tiered screening, 900 top ranked molecules (C_Score) were then subjected to molecular clustering. The best C_score compound from each cluster was brought forward for biological assay, and subsequently three compounds showed activity in FP and/or TR-FRET.

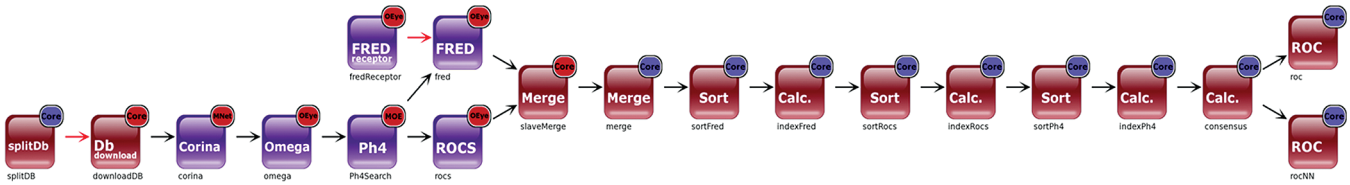

Figure 5. PyPe tiered screening protocol. Various components of the PyPe tiered screening protocol are arranged in a linear or parallel topology. splitDB splits or distributes stored database compounds evenly to the compute nodes. downloadDB downloads compounds from the database on each compute node after the component splitDB carries out data load balancing. Subsequently, CORINA and OMEGA convert database compounds from SMILES to 3D molecular representations. MOE pharmacophore search creates a pharmacophore screening model via an automated consensus query (or manually generated Ph4 input file) and filters the database according to the pharmacophore query used. After this step, molecules that clear the pharmacophore are passed to FRED and ROCS for docking and shape-based superimposition query generation, respectively. The slaveMerge component carries out data merging on compute nodes, while merge gathers together all incoming files into a single file. After merging, compounds are sorted and indexed separately for FRED, ROCS, and MOE Ph4 and a consensus score is calculated by the calc component. ROC curve output analysis is carried out using the ROC component in PyPe. Results are exported in multiple formats for analysis.

Table 1. Individual and C_score Ranking of Active Compounds[a]

compd	SPECS code	MOE Ph4 rank	FRED rank	ROCS rank	C_Score	C_Score rank
1	AN-698/15136006	223/900	111/900	134/900	156.0	12/900
2	AK-968/41923327	146/900	68/900	334/900	182.7	21/900
3	AF-399/40992009	810/900	185/900	631/900	542.0	641/900

[a]Listed above is the rank of hit compounds in individual screening techniques (MOE pharmacophore, FRED, and ROCS) versus the rank designated by consensus score (C_Score).

scored subset. The highest ranked compound in each of the clusters was purchased for biological assay. To judge the benefits of tiered screen applicability, the output ranks of **1**, **2**, and **3** were analyzed for individual screening techniques and compared to that of the tiered screening C_score (Table 1). In the cases of **1** and **2**, the C_score rank outperforms those rankings obtained from MOE pharmacophore, FRED or ROCS alone. The C_score performance of **3** outperforms only the pharmacophore; however, the high consensus ranking of the compound does bestow a measure of greater confidence to its selection for evaluation in assay. Through C_score ranking, both **1** and **2** were placed in enriched areas of the PyPe tiered screen output list (top 1.3% and 2.3%, respectively). This compared favorably to placement seen by individual screening methods. The C_score of **3** performed poorly compared to other hit compounds and individual method ranks. Aside from its C_score, the prioritization of **3** for biological testing arises from the application of the clustering applied to the tiered screened data set. As a highest ranked diverse structure (by molecular similarity), **3** is advanced not only because

dx.doi.org/10.1021/jm300068n | J. Med. Chem. 2012, 55, 4978−4989

of consensus scoring but also because of scaffold diversity, essential in this instance where scaffold hopping away from the TZD warhead is paramount.

Competitive Binding of Virtual Screening Hits. To examine potential biological activity of virtual screening "hits", initial assessment involved testing the compounds at a single-point concentration (100 μM) in fluorescence polarization (FP) assay. From 20 compounds assayed, three compounds (**1**, **2**, **3**) displayed competitive binding to the PPARγ-LBD comparable to that of the control (rosiglitazone, 100 μM). Consequently, eight-point dose response curves were constructed to determine EC_{50} values for these putative hits. From FP dose response curves, **1** was shown to bind PPARγ-LBD with an EC_{50} of 325 ± 80 nM. **2** and **3** displayed EC_{50} values of 5.45 ± 1.2 μM and 2.4 ± 0.8 μM, respectively (Figure 3). Positive control displayed activity in line with that previously reported in the literature.[24] **1**, **2**, and **3** displayed competitive binding activities in the mid-nanomolar to low micromolar range, with **1** displaying the strongest affinity for PPARγ-LBD.

From initial FP investigations, the competitive binding characteristics of the three hit compounds were determined using an alternative complementary technique. Time resolved fluorescence resonance energy transfer (TR-FRET) is a recognized method for overcoming interference from compound autofluorescence or light scatter from precipitated compounds.[24] In order to further and better qualify results obtained from FP and to rule out any possible false positive data from compound autofluorescence or insolubility, **1**, **2**, and **3** were assayed using TR-FRET. All three compounds definitively demonstrated the competitive binding characteristics displayed in FP. In each case, positive control compounds were included for experimental control and calculated EC_{50} values were in agreement with values referenced in the kit literature[24] (Table 2).

In order to determine the PPAR isotype selectivity of the compounds, **1**, **2**, and **3** were also tested in TR-FRET competitive binding assays against PPARα- and PPARδ-LBDs (Table 2, Figure 6). Compounds were initially assessed at two concentrations (50 and 100 μM) to ascertain potential competitive binding to the PPARα-LBD or PPARδ-LBD. In the case of **1**, the compound did not display statistically significant binding to either the PPARα or PPARδ isotypes ($P < 0.05$). These results suggest that **1** displays a specific high affinity for the γ isotype of the PPAR family. Compound **2** demonstrated appreciable binding to all three isotypes as determined by TR-FRET competitive binding ($\gamma/\alpha/\delta$ ratio = 1:2:4) indicating a pan-PPAR activity profile. Compound **3** displayed competitive binding to both the γ and δ PPAR isoforms (γ/δ ratio = 1:10.8). Additionally, **3** did not show effective displacement of pan-PPAR fluormone at ≤100 μM, positioning it as a dual PPARγ/δ scaffold.

PPARγ TR-FRET Activation Reporter Assay. Consequent from on-target biochemical validation of compounds **1**, **2**, and **3** competitive binding to PPARγ-LBD, activity was assessed in a cell based TR-FRET activation reporter assay (Figure 7). Over the compound concentrations assayed (10 nM to 10 μM), all compounds displayed dose-dependent agonism of PPARγ-LBD within the cellular reporter assay. Compound **1** retained the highest affinity toward the receptor (EC_{50} = 0.467 ± 0.139 μM), while both compounds **2** and **3** demonstrated higher affinities within the activation reporter assay compared to that shown in the on-target competitive binding studies (EC_{50} = 0.682 ± 0.357 μM and 0.594 ± 0.059 μM, respectively). Interestingly, in comparison to rosiglitazone, both compounds **2** and **3** did not induce full receptor activation at the maximal concentrations assayed (Table 2). Compound **1** showed comparable activation to rosiglitazone within the concentration window assayed. All experimental compounds were also assayed for activity as PPARγ antagonists and failed to abrogate rosiglitazone induced PPARγ activation at ≥10 μM (data not shown). In view of these findings, we suggest that **1**, **2**, and **3** show differing degrees of agonism against PPARγ-LBD within this TR-FRET cell-based activation reporter assay.

Compound Chemodiversity. To quantify novelty of newly identified compounds, the structural similarity of **1**, **2**, and **3** was contrasted to that of the 22 PPAR actives used in the ligand training set (see Supporting Information Table S1). As documented in Table 3, all compounds showed diversification from the established chemical scaffolds contained within the ligand set. As determined by Tanimoto coefficient (varying settings), none of the new compounds exhibit a similarity of >0.322 to those known ligands contained in the data set. Furthermore, structural similarity was calculated for each novel compound against the DUD PPARγ active set. Across the different fingerprint schemes used in Pipeline Pilot (FCFP4/6 and ECFP4/6), the average calculated Tanimoto coefficient for **1**, **2**, and **3** was 0.198, 0.245, and 0.188, respectively. To further quantify novelty, all hit compounds were screened (similarity searching) against established drug databases to compare chemotype originality to known PPAR modulators (see Supporting Information Table S4), again confirming chemotype novelty. We conclude that the use of such a tiered screening protocol for identification of novel PPAR scaffolds has delivered a scheme capable of discovering structurally dissimilar active chemotypes.

DISCUSSION

In summary, the work presented has showcased the ability of a custom built tiered screening protocol to computationally identify novel scaffolds for PPARγ. Implementation of an equally weighted consensus scoring function across ligand- and structure-based drug discovery techniques focused an initial large database size to that more amenable to further investigations. Through biochemical assay, virtual hits were experimentally tested, resulting in the discovery of three novel small molecule PPAR scaffolds, with activities spanning from low micromolar to mid-micromolar concentration ranges. **1** displayed specific binding within tested concentrations against PPARγ, with an affinity approximately double that of rosiglitazone (EC_{50} of 215 nM vs 120 nM). In contrast, **2** showed differing levels of affinity for three PPAR receptor subtypes. Interestingly, **2** displayed preferential binding to PPARγ but retained potency (decreasing) against PPARα and PPARδ, respectively. It has been postulated that agonism of all three PPAR subtypes could have benefits in a broad spectrum of metabolic diseases.[26] Previous work on PPAR pan-agonist development has revealed compounds with both similar and differing ratios of PPAR isotype preferential binding.[27,28] Compound **3** was shown to have dual affinity for both PPARγ and PPARδ. On the basis of the intricate involvement of PPARγ/δ on lipid metabolism, dual target modulation has been suggested as a potentially beneficial approach toward treatment of hyperlipidemia, insulin resistance, and attenuation of atherogenesis. Indeed, several studies have shown positive preclinical data emanating from dual PPARγ/δ targeting treatments.[29,30] In further support of compound activity, **1**, **2**, and **3** were shown to display varying degrees of agonism within a PPARγ TR-FRET activation reporter assay. This result shows the ability of all

Table 2. Structures, EC_{50}, and 2D Descriptors for 1, 2, 3, and Agonist Controls[a]

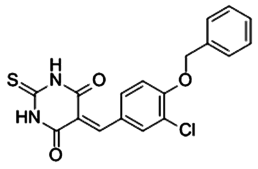

MDG 548

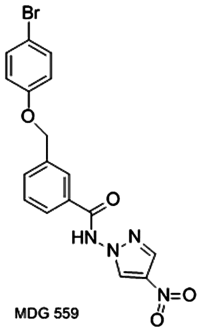

MDG 559

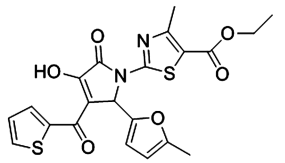

MDG 582

	EC_{50} (μM)				EC_{50} (μM)					
compd	PPARγ FP	PPARγ TR-FRET	GeneBLAzer PPARγ 293H DA cell-based assay (μM)	maximum response ratio, %	PPARα TR-FRET	PPARδ TR-FRET	log P(O/W)	SlogP	reactive	opr_violation
1	0.325 ± 0.08	0.215 ± 0.02	0.467 ± 0.139	91.6 ± 3.2	na	na	3.114	3.010	0	0
2	5.45 ± 1.2	5.45 ± 2.56	0.682 ± 0.357	68.7 ± 3.4	11.4 ± 4.2	21.0 ± 6.7	3.708	3.783	1	0
3	2.40 ± 0.8	2.40 ± 1.5	0.594 ± 0.059	77.5 ± 0.8	na	26.0 ± 3.6	2.387	4.469	0	1
rosiglitazone	0.190 ± 0.11	0.120 ± 0.06	0.0024 ± 0.0017		na	na	2.621	2.499	0	0
GW1929	0.026 ± 0.004	0.0037 ± 0.0012			55.3 ± 6.3	na	5.228	4.936	0	2
GW7647	na	na			0.0018 ± 0.0004	na	8.020	7.279	0	2
GW0742	na	na			0.920 ± 0.024	0.0029 ± 0.001	5.947	6.918	0	1

[a] EC_{50} values determined by fluorescence polarization, time resolved fluorescence resonance energy transfer, and GeneBLAzer PPARγ 293H DA cell-based assay. Maximum response ratio is calculated as percentage of response ratio compared to rosiglitazone (10.0 μM). na: no statistically significant activity displayed at ≥100 μM (two-way ANOVA, Bonferroni post-test, $P < 0.05$). Where applicable, values represent data ± SEM. 2D descriptors were calculated using MOE (version 2011.10, Montreal, Canada). log P(O/W): log of the octanol/water partition coefficient (including implicit hydrogens). SlogP: log of the octanol/water partition coefficient (including implicit hydrogens). Reactive: indicator of the presence of reactive groups. A non-zero value indicates that the molecule contains a reactive group. The table of reactive groups is based on the Oprea set.[25] opr_violation: the number of violations of Oprea's leadlike test.[25]

dx.doi.org/10.1021/jm300068n | J. Med. Chem. 2012, 55, 4978−4989

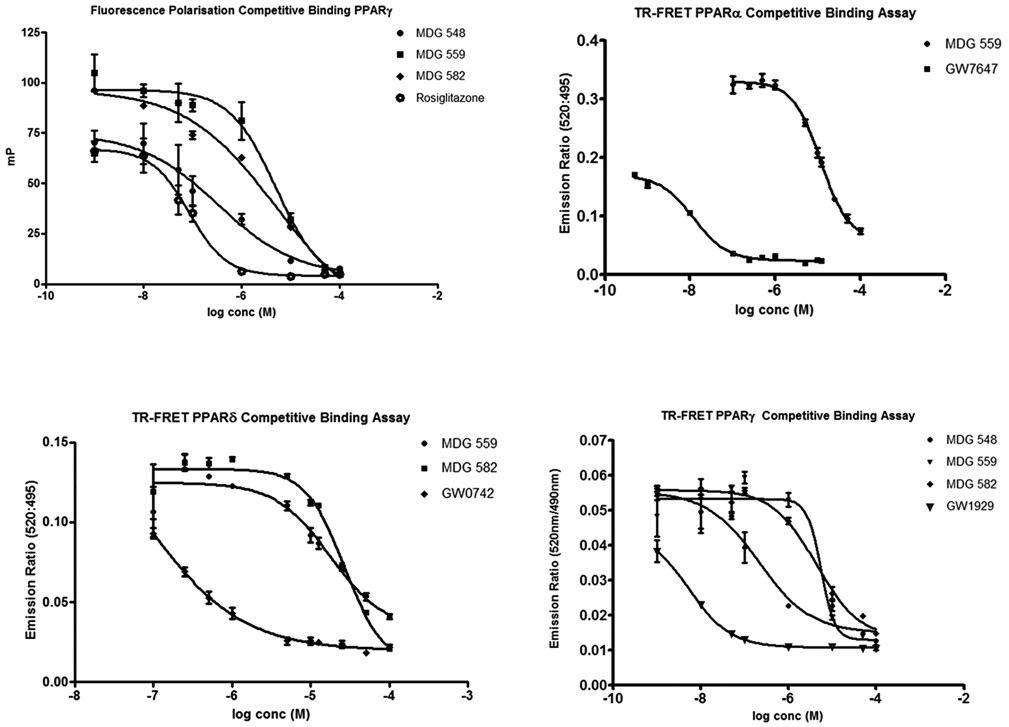

Figure 6. FP and TR-FRET competitive binding assay for PPAR isotypes. Positive controls were used in each experiment to judge experimental efficacy: PPARγ, rosiglitazone/GW1929; PPARα, GW7647; PPARδ, GW0742. Each point represents triplicate data from at least two independent experiments. Error bars represent the standard error of the mean (SEM). Assay Z' factors are as follows: FP PPARγ, 0.82; TR-FRET PPARα, 0.61; TR-FRET PPARδ, 0.56; TR-FRET PPARγ, 0.79.

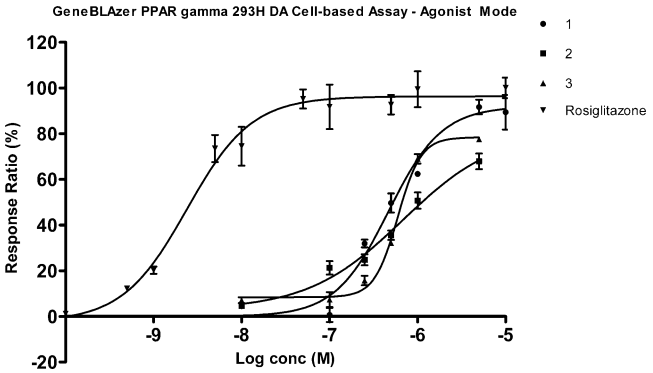

Figure 7. GeneBLAzer PPARγ 293H DA cell-based assay: TR-FRET based activation reporter assay for **1**, **2**, **3**, and rosiglitazone. Concentrations ranged from 0.1 to 10 000 nM. Response ratio is calculated as percentage of maximum emission ratio observed at 10 μM rosiglitazone. Each point represents triplicate data from at least two independent experiments. Error bars represent the standard error of the mean (SEM): assay Z' factor, 0.91.

Table 3. Tanimoto Coefficient Scores for 1, 2, and 3 against Group A PPAR Ligands[a]

compd	FCFP 4	FCFP 6	ECFP 4	ECFP 6
1	0.258	0.180	0.192	0.195
2	0.322	0.143	0.227	0.169
3	0.209	0.139	0.202	0.128

[a]Reported is the highest degree of similarity shown between a training set ligand and novel screening hits for each of four fingerprint schemes used (i.e., FCFP4, FCFP6, ECFP4, ECFP6).

compounds to induce PPARγ activation within a cellular system and diminishes the potential for reporting on screening artifacts.

In terms of the computational strategies employed and evident from the chemical diversity of compounds discovered, the tiered PPAR protocol is able to explore vast regions of chemical space in a manner that is unbiased by any individual computational screening technique. Retrieved actives typically displayed higher ranks in tiered screening hit lists versus that of MOE pharmacophore, FRED, or ROCS alone. Structural similarity studies have shown the ability of the protocol to identify novel PPAR chemotypes. It is our intention to further investigate the biological activity of compounds showing competitive binding against the targets of interest, including full characterization of their effects in diverse cellular models. Promising hits will be subject to analogue/substructure exploration to build informative structure−activity relationship data and improve lead druglikeness. Also, the utility of the integrated tiered screening protocol used here will be further explored across other members of the nuclear receptor superfamily.

METHODS

PPARγ Receptor Selection, Preprocessing, and PLIF Analysis. Seventy-three PPARγ X-ray crystal structures were downloaded from the RCSB Protein Data Bank.[31] To reduce the list size and implement a systematic PDB selection process, several exclusion criteria were applied to the structures: (1) Only structures with cocrystallized druglike compounds were chosen. (2) No mutated protein structures were included. (3) Repeated ligand−protein complexes were excluded. Structures were then imported in MOE (version 2010.10, Montreal, Canada), and PPARγ-LBD repeats, cocrystallized biocomplexes (co-regulators, DNA, etc.), water molecules, and repeated ligands were removed. The proteins were superimposed using MOE's Protein Align function (default) in order to carry out protein ligand interaction fingerprint (PLIF) analysis. In brief, PLIF is a method for analyzing the interactions between ligands and proteins using a fingerprint scheme that allows for a convenient structural differentiation between

dx.doi.org/10.1021/jm300068n | J. Med. Chem. 2012, 55, 4978−4989

complexes. Protein−ligand interaction profiles were analyzed, and PPARγ complexes were segmented into two groups (group A and group B) dependent on the ligand−protein interaction profiles observed.

Database of Useful Decoys (DUD). A key metric of molecular screening techniques is active compound enrichment among top-ranking hits. In order to avoid bias in model validation, decoys contained in a database should resemble ligands physically so that enrichment is not simply a separation of gross features and yet should be chemically distinct from them so that they are unlikely to be binders. The Database of Useful Decoys (DUD) is an assembled database of target specific actives and decoys.[32] On average, each protein target has 36 decoys per active molecule that are physiochemically similar, but topologically distinct, to target actives. Throughout this study, the PPARγ DUD set was used to assess a screening model's efficacy at separating known actives from presumed decoy compounds.

Receiver Operator Curve (ROC) Analysis. A common metric used for judging the significance of a hypothesis is to evaluate how a model discriminates between active molecules and decoys. In a ROC curve, the true positive rate is plotted as a function of the false positive rate. Each point on the ROC curve represents a sensitivity/specificity pair. An ideal test with perfect discrimination (no overlap in the two distributions) has a ROC plot that passes through the upper left corner (100% sensitivity and specificity).[33] Usage of ROCS as a metric of virtual screening utility assessment has previously been discussed and advocated.[20,21]

PyPe. PyPe is a cluster side parallel platform for vHTS that takes advantage of current computational tools and high performance computing technologies. In advancing PyPe, we create a homogeneous parallel system that dramatically decreases the turnaround time of large computational tasks with minimum setup. The PyPe platform was designed to unify the interfaces between diverse applications and users. Python/MPI (mpi4py) was used to wrap tools from CCG, OpenEye, Molecular Networks, MySQL, ReportLab, Gnuplot and R.

PyPe was developed using a modular design that is easily maintained using the distributed version control software Git. A modular design has key advantages such that each subunit can be easily tested (unit or regression) and makes the learning curve for the user and developer easier. PyPe was designed for a high performance computing environment, and all computational intensive calculations run in parallel. PyPe is fully extendable using a plug-in type model. New code or third party applications can be very easily added to create new components. PyPe converts a heterogeneous working environment into a homogeneous one where the interface to numerous and diverse codes is consistent. Protocols within PyPe are customizable by the user using an xml schema. All end points from calculations can be output in PDF format.

Conformer Generation: Method Comparison and Validation. As inclusion of a bioactive conformation in ligand data sets is of paramount importance in virtual screening, molecular conformational searching is routinely carried out, as often compounds are stored as a 1D string or flat 2D descriptions. For the purposes of this study, three methods of conformer generation were used and directly compared to assess their suitability in this screening campaign. First, group A and group B ligands were input to CORINA (version 3.46, Erlangen, Germany) to generate single 1D−3D structures (default settings).[34] In MOE, stochastic and LowModeMD conformer generation techniques were studied. In short, the stochastic search method generates conformations by randomly rotating all bonds (including ring bonds) and randomly inverting tetrahedral centers followed by an all-atom energy minimization. LowModeMD search method generates conformations using a short (∼1 ps) run of molecular dynamics (MD) at constant temperature followed by an all-atom energy minimization. For simplification, default settings were implemented in both methods (iteration limit of 10 000). Conformer exploration was also carried out using OMEGA (version 2.3.2, OpenEye, Sante Fe, NM).[35] OMEGA generates conformational ensembles using predefined rules that are applied to two independent components: model building and torsion driving. As with MOE methods, default settings were retained for OMEGA, with the exception of the max confgen and max confs settings (set at 50 000 and 10 000, respectively). In order to compare generated conformers to the validation ligand bioactive pose for each group ligand, a custom SVL (scientific vector language) script (Chemical Computing Group Exchange)[36] was used to superimpose each conformer to the ligand crystal pose. The degree of superimposition was calculated by root mean square deviation (rmsd) comparison.

OMEGA Parametrization and Setting Validation. To ascertain if deviation from default settings in OMEGA was important for conformer generation, the effect of select parameter variation was investigated. Previous ligand analysis showed that on average PPARγ modulators are relatively flexible molecules containing 9.7 rotatable bonds. In view of this information, the max confs parameter was designated as holding potential importance in the exploration of conformer space for this virtual screening campaign.

Group A ligands were extracted from their cocomplexed structures and saved in SDF (structure data format) file. The max confs setting was incrementally varied from default (100−10000). The max confgen and rms settings were fixed at 50 000 and 0.5, respectively, to aid in initial model simplicity. Calculation of conformer rmsd to bioactive conformation was carried out using the custom SVL script previously discussed (mol_rmsd.svl).

Pharmacophore Model Creation. Pharmacophore models were created and iterated using the pharmacophore query editor function in MOE (version 2010.10, Montreal, Canada). Two methods for pharmacophore creation were analyzed, namely, (a) consensus pharmacophore creation using the group B ligand data set and (b) manual query built using the PPARγ agonist rosiglitazone as the template ligand. In both cases, the PCH pharmacophore scheme was used (default settings). In the manually created model, the query was varied via adjustment of pharmacophore sphere radii, addition of exclusion volumes around ligand binding area, defining of essential/nonessential features, and inclusion of a partial match stipulation to the query (see Supporting Information Table S3). Pharmacophore hypothesis performance was assessed by comparing the retrieval rate of actives vs decoys in the PPARγ DUD ligand data set. In tandem with this, ROC curve analysis for pharmacophore models was carried out on the same ligand set.

FRED: Receptor Preparation and Method Validation. Fast rigid exhaustive docking (FRED, version 2.2.5, OpenEye, Sante Fe, NM)[19] performs exhaustive docking by enumerating rigid rotations and translations of each given database conformer within the target active site. Shape based filters are used to rapidly filter compounds in the database that are not complementary to the binding site. Poses that pass the shape fitting process can then be ranked by multiple scoring function algorithms in the screening process. In order to ascertain the usability of FRED in the virtual screening protocol, its ability to successfully re-dock the bioactive conformation of a cocrystallized PPAR agonist (rosiglitazone, PDB code 1FM6[37]) was studied. Using FRED receptor (version 2.2.5, OpenEye, Sante Fe, NM), the protein/ligand moieties of the complex were defined and mutable residue states were left at default. Constraints were placed on residues Ser289 and Tyr473 (hydrogen bond acceptor and donor features, respectively).

To assess the performance of different scoring functions used in FRED, a molecular database of rosiglitazone conformers (n = 1000) created by OMEGA was seeded with the bioactive conformation of the compound. The complete database was then docked into the preprepared PPARγ-LBD receptor and the ranked output lists for each scoring function visualized using VIDA (version 4.0.3, OpenEye, Sante Fe, NM). Comparison of the rmsd of output poses to the bioactive conformation was carried out using the previously discussed custom SVL script in MOE. Subsequent to the initial component validation, the ability of FRED to discriminate between PPARγ actives and decoys was determined using the DUD set of compounds for the PPARγ receptor. Protocol performance was assessed using standard receiver operating characteristic (ROC) curve analysis.

ROCS: Query Creation and Validation. Rapid overlay of chemical structures (ROCS, version 2.4.1, OpenEye, Sante Fe, NM) is used to perform large scale 3D database searches by using a superposition method that finds compounds similar to known actives.[38] Molecules are aligned by a solid-body optimization process that

maximizes the overlap volume between them. With a view to avoiding a thiazolidinedione bias in the virtual screening protocol, a query for ROCS was created using the tyrosine based PPARγ agonist GI262570 (PDB code 1FM9[37]). On the basis of a chemically distinct scaffold from TZDs, this variation was introduced to further test the performance of the virtual screening protocol used. GI262570 also possesses a larger volume than typical TZD scaffolds, allowing for accommodation of larger potential actives to pass this stage of the screen. The native ligand pose was extracted from the source PDB file, and ROCS validation (version 2.4.1, OpenEye, Sante Fe, NM) was carried out using the PPAR DUD set previously discussed (default). Scoring function performance was assessed by ROC curve analysis.

Tiered Screening: Application and Validation. From parametrization and validation of individual virtual screening components (Figure 3), the performance of the protocols combined within the tiered screening model was analyzed. A PyPe protocol implementing tiered screening (Figure 5) was employed in a custom built pipeline with multiple components run in parallel in order to decrease the computational turnaround time and facilitate the spread of individual software calculations over multiple CPUs. From individual component analysis, the DUD PPARγ ligand data set was used to validate the protocol and to examine the computational performance of the tiered screen. All components were run using validated parameters previously detailed.

Database Screening. Virtual screening for novel PPARγ scaffolds was performed on the SPECS vendor database[39] (approximately 200 000 compounds). In order to reduce the initial data set size, a series of physiochemical descriptors were applied to the database as inclusion criteria. Typical descriptor values were calculated from a series of 22 known PPAR ligands and upper/lower cutoff limits applied to the filter process (Table 4).

Table 4. Calculated Physiochemical Descriptors of a Set of Known PPARγ Ligands[a]

MOE descriptor	min	max	mean	standard deviation	range
MW	317.40	590.74	469.65	76.09	300−550
B_rotN	4.0	14	9.77	2.71	4−12
a_acc	0	5	2.77	1.23	0−5
a_don	0	2	0.36	0.66	0−2
log *P*(O/W)	2.62	9.36	6.64	1.76	2−8

[a]In order to construct a prescreening database of molecules, a series of physiochemical descriptor filters were applied to the data set. Min/max settings were determined from a set of 22 PPARγ agonists documented in the literature (data not shown). Descriptors were calculated in MOE. MW: molecular weight. B_rotN: number of rotatable bonds. a_acc/don: number of hydrogen bond acceptor/donator atoms. log *P*(O/W): log of partition coefficient of octanol/water.

Molecular Clustering. After application of the virtual screening protocol on the reduced SPECS database, the top 900 hit molecules were further subjected to a molecular clustering protocol in order to prioritize compounds for biological testing. By use of a custom built Pipeline Pilot protocol (version 8.5, Accelrys, San Diego, CA), hit molecules were grouped into clusters using the FCFP_4 fingerprint (average number per cluster, 45; number of clusters, 20). FCFP_4 fingerprints encode six general atom types with the numeral value denoting the diameter of the circular substructure. The highest consensus scoring (C_Score) molecules from each molecular cluster were advanced to on-target biochemical testing (Table 1).

Chemical Similarity. To deduce the similarity between **1**, **2**, **3** and training set compounds, a custom structural similarity protocol was created in Pipeline Pilot (version 8.5, Accelrys, San Diego, CA). Similarity coefficient used was Tanimoto, and predefined settings were FCFP4, FCFP6, ECFP4, and ECFP6. All molecular structures were checked for correct representation prior to similarity calculations.

Biological Methods. General Procedures. All compounds used for virtual screening and biological testing were commercially available from SPECS.[39] All positive controls (rosiglitazone, GW1929, GW0742, and GW7647) were sourced from Sigma Aldrich (St. Louis, MO). Purities of compounds were assessed by a combination of ^{1}H NMR and LCMS and were found to be >95%.

Fluorescent Polarization Competitive Binding Assay. PolarScreen PPAR competitor assay kit (PV3355, Invitrogen, Carlsbad, CA) was used to assess the competitive binding characteristics of virtual hit compounds against PPARγ-LBD. Experiments were carried out in line with guidelines specified by the supplier. In short, 2× compound/control solutions were made up in PPAR Green screening buffer (2% DMSO) and an amount of 20 μL was added to a microwell plate (Corning, NY, U.S.) along with 20 μL of 2× PPAR-LBD/Fluormone complex. Final concentration of DMSO in each well was 1%. Plates were stored in the dark at room temperature for 2 h prior to reading on a PHERAstar Plus HTS microplate reader (BMG LabTech). On each plate a vehicle control (1% DMSO in buffer), maximum mP control (20 μL of PPAR-LBD/Fluormone complex + 20 μL of complete assay buffer), and minimum mP control (20 μL of Fluormone + 20 μL of complete assay buffer) were included. Positive controls were included in each experimental run (rosiglitazone and/or GW1929). The mP values were analyzed using GraphPad Prism (version 5.01, San Diego, CA) and curves fit using sigmoidal dose-response equation (varying slope) to determine EC_{50} values. Data points represent triplicate averages over two independent experiments. Error bars show standard error of the mean (SEM) of replicate wells.

LanthaScreen TR-FRET PPAR Competitive Binding Assay. LanthaScreen TR-FRET PPAR competitive binding assay kit (PPARγ-PV4894, PPARα-PV4892, PPARδ-PV4893, Invitrogen, Carlsbad, CA) was used as specified by the supplier documentation. In brief, 2× test compound/control solutions were made up in TR-FRET PPAR assay buffer (2% DMSO) and an amount of 20 μL was added to a microwell plate (Corning, NY, U.S.). After compound addition, 10 μL of 4× Fluormone pan-PPAR Green and 10 μL of 4× PPAR-LBD/Tb-anti-GST Ab were added to each test well. Plates were stored in the dark at room temperature for 2 h prior to reading on a PHERAstar Plus HTS microplate reader (BMG LabTech). On each plate a negative control, representing 0% displacement, was included (20 μL of 2× test compound solvent (TR-FRET PPAR assay buffer, 2% DMSO)) + 10 μL of 4× Fluormone pan-PPAR Green + 10 μL of 4× PPARγ-LBD/Tb-anti-GST Ab). Positive controls were included in each experimental run (rosiglitazone and/or GW1929 for PPARγ, GW7647 and GW0742 for PPARα and PPARδ, respectively). TR-FRET ratio was calculated by dividing the emission signal at 520 nm by the emission signal at 495 nm. Data values were analyzed using GraphPad Prism (version 5.01, San Diego, CA) and curves fit using sigmoidal dose-response equation (varying slope) to determine EC_{50} values. Data points represent triplicate averages over two independent experiments. Error bars show SEM of replicate wells.

GeneBLAzer PPARγ 293H DA Cell-Based Assay. GeneBLAzer PPARγ 293H DA cell-based assay (K1419, Invitrogen, Carlsbad, CA) and cell medium reagents were used as specified by the supplier documentation. In brief, PPARγ 293H DA cells were plated at 30 000 cells/well in a 384-well plate and stimulated with test compounds and suitable controls (rosiglitazone) at varying concentrations for approximately 16 h (0.1% DMSO final concentration). Cells were then loaded with LiveBLAzer-FRET B/G substrate for 2 h. Fluorescence values at 460 and 530 nm were obtained using a SpectraMax M2e fluorescence plate reader (Molecular Dimensions, Bath, U.K.). Data values were analyzed using GraphPad Prism (version 5.01, San Diego, CA) and curves fit using sigmoidal dose-response equation (varying slope) to determine EC_{50} values. Data points represent triplicate averages over two independent experiments. Error bars show SEM of replicate wells.

■ ASSOCIATED CONTENT

Ⓢ Supporting Information

Group A/B ligand set, OMEGA parametrization, pharmacophore model testing data, experimental controls for artificial

inhibition, compound novelty data, and two ChemDraw files containing chemical structures. This material is available free of charge via the Internet at http://pubs.acs.org.

AUTHOR INFORMATION

Corresponding Author

*Phone: +353(1)8963527. E-mail: lloyddg@tcd.ie.

Present Address

[§]Molecular Design Group, School of Biochemistry and Immunology, Trinity Biomedical Sciences Institute, Trinity College Dublin, Dublin 2, Ireland.

Notes

The authors declare no competing financial interest.

ACKNOWLEDGMENTS

The authors acknowledge financial support from the Trinity Postgraduate Research Studentship (D.K.N.), Enterprise Ireland (G.C.), and the Irish Research Council for Science, Engineering and Technology (IRCSET) (M.B.P.). We thank the software vendors for their continuing support of such academic research efforts, in particular the contributions of Accelrys, the Chemical Computing Group, and OpenEye Scientific, which significantly underpinned the work performed in this study. Also acknowledged is the support and provisions of the Trinity Centre for High Performance Computing (TCHPC) and the Irish Centre for High-End Computing (ICHEC). The Trinity Biomedical Sciences Institute is supported by a capital infrastructure investment from Cycle 5 of the Irish Higher Education Authority's Program for Research in Third Level Institutions (PRTLI). ICHEC is supported through funding from Science Foundation Ireland. Authors also thank Prof. Clive Williams' group for their invaluable insights into the biological validation aspects of the work and Prof. Martin Caffrey's group for kind use of their equipment.

ABBREVIATIONS USED

AUC, area under the curve; DUD, Database of Useful Decoys; FP, fluorescence polarization; FPR, false positive rate; FRED, fast rigid exhaustive docking; LBD, ligand binding domain; MD, molecular dynamics; NPV, negative predictive value; PCH, polar−charged−hydrophobic; PLIF, protein ligand interaction fingerprint; PPAR, peroxisome proliferator-activated receptor; PPRE, peroxisome proliferator-activated receptor response element; PyPe, parallel Python Pipeline; rmsd, root mean square deviation; ROC, receiver operating characteristic; ROCS, rapid overlay of chemical structures; RXR, 9-*cis*-retinoic acid receptor; SEM, standard error of the mean; SVL, scientific vector language; TR-FRET, time resolved fluorescence resonance energy transfer; TZD, thiazolidinedione

REFERENCES

(1) Nuclear Receptors Nomenclature Committee. A unified nomenclature system for the nuclear receptor superfamily. *Cell* **1999**, *97*, 161−163.

(2) Zieleniak, A.; Wojcik, M.; Wozniak, L. A. Structure and physiological functions of the human peroxisome proliferator-activated receptor gamma. *Arch. Immunol. Ther. Exp.* **2008**, *56*, 331−345.

(3) Berger, J.; Moller, D. E. The mechanisms of action of PPARs. *Annu. Rev. Med.* **2002**, *53*, 409−435.

(4) Bernardo, A.; Minghetti, L. PPAR-gamma agonists as regulators of microglial activation and brain inflammation. *Curr. Pharm. Des.* **2006**, *12*, 93−109.

(5) Bordet, R.; Gele, P.; Duriez, P.; Fruchart, J. C. PPARs: a new target for neuroprotection. *J. Neurol., Neurosurg. Psychiatry* **2006**, *77*, 285−287.

(6) Bright, J. J.; Walline, C. C.; Kanakasabai, S.; Chakraborty, S. Targeting PPAR as a therapy to treat multiple sclerosis. *Expert Opin. Ther. Targets* **2008**, *12*, 1565−1575.

(7) Chaturvedi, R. K.; Beal, M. F. PPAR: a therapeutic target in Parkinson's disease. *J. Neurochem.* **2008**, *106*, 506−518.

(8) Cheng, A. Y.; Leiter, L. A. PPAR-alpha: therapeutic role in diabetes-related cardiovascular disease. *Diabetes, Obes. Metab.* **2008**, *10*, 691−698.

(9) Kersten, S.; Desvergne, B.; Wahli, W. Roles of PPARs in health and disease. *Nature* **2000**, *405*, 421−424.

(10) Nevin, D. K.; Lloyd, D. G.; Fayne, D. Rational targeting of peroxisome proliferating activated receptor subtypes. *Curr. Med. Chem.* **2011**, *18*, 5598−5623.

(11) Choi, J.; Ko, Y.; Lee, H. S.; Park, Y. S.; Yang, Y.; Yoon, S. Identification of (beta-carboxyethyl)-rhodanine derivatives exhibiting peroxisome proliferator-activated receptor gamma activity. *Eur. J. Med. Chem.* **2010**, *45*, 193−202.

(12) Lin, C. H.; Peng, Y. H.; Coumar, M. S.; Chittimalla, S. K.; Liao, C. C.; Lyn, P. C.; Huang, C. C.; Lien, T. W.; Lin, W. H.; Hsu, J. T.; Cheng, J. H.; Chen, X.; Wu, J. S.; Chao, Y. S.; Lee, H. J.; Juo, C. G.; Wu, S. Y.; Hsieh, H. P. Design and structural analysis of novel pharmacophores for potent and selective peroxisome proliferator-activated receptor gamma agonists. *J. Med. Chem.* **2009**, *52*, 2618−2622.

(13) Liu, Q.; Zhang, Y. Y.; Lu, H. L.; Li, Q. Y.; Zhou, C. H.; Wang, M. W. Rhodanine derivatives as novel peroxisome proliferator-activated receptor gamma agonists. *Acta Pharmacol. Sin.* **2007**, *28*, 2033−2039.

(14) Vidovic, D.; Busby, S. A.; Griffin, P. R.; Schurer, S. C. A combined ligand- and structure-based virtual screening protocol identifies submicromolar PPARgamma partial agonists. *ChemMedChem* **2011**, *6*, 94−103.

(15) Onnis, V.; Kinsella, G. K.; Carta, G.; Jagoe, W. N.; Price, T.; Williams, D. C.; Fayne, D.; Lloyd, D. G. Virtual screening for the identification of novel nonsteroidal glucocorticoid modulators. *J. Med. Chem.* **2010**, *53*, 3065−3074.

(16) Yang, Y.; Carta, G.; Peters, M. B.; Price, T.; O'Boyle, N.; Knox, A. J. S.; Fayne, D.; Williams, D. C.; Megan, M. J.; Lloyd, D. G. "tieredScreen"—layered virtual screening tool for the identification of novel estrogen receptor alpha modulators. *Mol. Inf.* **2010**, 421−430.

(17) Caboni, L.; Kinsella, G. K.; Blanco, F.; Fayne, D.; Jagoe, W. N.; Carr, M.; Williams, D. C.; Meegan, M. J.; Lloyd, D. G. "True" antiandrogens-selective non-ligand-binding pocket disruptors of androgen receptor−coactivator interactions: novel tools for prostate cancer. *J. Med. Chem.* **2012**, *55*, 1635−1644.

(18) Knox, A. J.; Meegan, M. J.; Carta, G.; Lloyd, D. G. Considerations in compound database preparation: "hidden" impact on virtual screening results. *J. Chem. Inf. Model.* **2005**, *45*, 1908−1919.

(19) *FRED*, version 2.6; OpenEye Scientific Software: Sante Fe, NM; www.eyesopen.com.

(20) Jain, A. N. Bias, reporting, and sharing: computational evaluations of docking methods. *J. Comput.-Aided Mol. Des.* **2008**, *22*, 201−212.

(21) Venkatraman, V.; Perez-Nueno, V. I.; Mavridis, L.; Ritchie, D. W. Comprehensive comparison of ligand-based virtual screening tools against the DUD data set reveals limitations of current 3D methods. *J. Chem. Inf. Model.* **2010**, *50*, 2079−2093.

(22) *Pipeline Pilot*; Accelrys: San Diego, CA; www.accelrys.com.

(23) *KNIME*; AG: Zurich, Switzerland; www.knime.com.

(24) *LanthaScreen TR-FRET Peroxisome Proliferator Receptor alpha Coactivator Assay Manual*; Invitrogen: Carlsbad, CA; tools.invitrogen.com/content/sfs/manuals/lanthascreen_PPARalpha_man.pdf.

(25) Oprea, T. I.; Gottfries, J.; Sherbukhin, V.; Svensson, P.; Kuhler, T. C. Chemical information management in drug discovery: optimizing the computational and combinatorial chemistry interfaces. *J. Mol. Graphics Modell.* **2000**, *18*, 512−524 , 541.

(26) Shearer, B. G.; Billin, A. N. The next generation of PPAR drugs: do we have the tools to find them? *Biochim. Biophys. Acta* **2007**, *1771*, 1082−1093.
(27) Artis, D. R.; Lin, J. J.; Zhang, C.; Wang, W.; Mehra, U.; Perreault, M.; Erbe, D.; Krupka, H. I.; England, B. P.; Arnold, J.; Plotnikov, A. N.; Marimuthu, A.; Nguyen, H.; Will, S.; Signaevsky, M.; Kral, J.; Cantwell, J.; Settachatgull, C.; Yan, D. S.; Fong, D.; Oh, A.; Shi, S.; Womack, P.; Powell, B.; Habets, G.; West, B. L.; Zhang, K. Y.; Milburn, M. V.; Vlasuk, G. P.; Hirth, K. P.; Nolop, K.; Bollag, G.; Ibrahim, P. N.; Tobin, J. F. Scaffold-based discovery of indeglitazar, a PPAR pan-active anti-diabetic agent. *Proc. Natl. Acad. Sci. U.S.A.* **2009**, *106*, 262−7.
(28) Oyama, T.; Toyota, K.; Waku, T.; Hirakawa, Y.; Nagasawa, N.; Kasuga, J. I.; Hashimoto, Y.; Miyachi, H.; Morikawa, K. Adaptability and selectivity of human peroxisome proliferator-activated receptor (PPAR) pan agonists revealed from crystal structures. *Acta Crystallogr., Sect. D: Biol. Crystallogr.* **2009**, *65*, 786−795.
(29) Johnson, T. E.; Holloway, M. K.; Vogel, R.; Rutledge, S. J.; Perkins, J. J.; Rodan, G. A.; Schmidt, A. Structural requirements and cell-type specificity for ligand activation of peroxisome proliferator-activated receptors. *J. Steroid Biochem. Mol. Biol.* **1997**, *63*, 1−8.
(30) Liu, K. G.; Lambert, M. H.; Leesnitzer, L. M.; Oliver, W., Jr.; Ott, R. J.; Plunket, K. D.; Stuart, L. W.; Brown, P. J.; Willson, T. M.; Sternbach, D. D. Identification of a series of PPAR gamma/delta dual agonists via solid-phase parallel synthesis. *Bioorg. Med. Chem. Lett.* **2001**, *11*, 2959−2962.
(31) RCSB Protein Data Bank. http://www.pdb.org.
(32) Huang, N.; Shoichet, B. K.; Irwin, J. J. Benchmarking sets for molecular docking. *J. Med. Chem.* **2006**, *49*, 6789−6801.
(33) Park, S. H.; Goo, J. M.; Jo, C. H. Receiver operating characteristic (ROC) curve: practical review for radiologists. *Korean J. Radiol.* **2004**, *5*, 11−18.
(34) *CORINA*; Molecular Networks: Erlangen, Germany; www.molecular-networks.com.
(35) *OMEGA*; OpenEye Scientific Software: Sante Fe, NM; www.eyesopen.com.
(36) *SVL Exchange*; Chemical Computing Group: Montreal, Canada, 2010; www.chemcomp.com.
(37) Gampe, R. T., Jr.; Montana, V. G.; Lambert, M. H.; Miller, A. B.; Bledsoe, R. K.; Milburn, M. V.; Kliewer, S. A.; Willson, T. M.; Xu, H. E. Asymmetry in the PPARgamma/RXRalpha crystal structure reveals the molecular basis of heterodimerization among nuclear receptors. *Mol. Cell* **2000**, *5*, 545−555.
(38) *ROCS*; OpenEye Scientific Software: Sante Fe, NM; www.eyesopen.com.
(39) SPECS home page (SPECS, Delft, The Netherlands). www.specs.net.